Child and adolescent development of the brain oscillatory activity during a working memory task

Carlos M. Gómez [a],[*], Vanesa Muñoz [a], Elena I. Rodríguez-Martínez [a], Antonio Arjona [a], Catarina I. Barriga-Paulino [b], Santiago Pelegrina [c]

[a] *Human Psychobiology Laboratory, Experimental Psychology Department, University of Sevilla, C/ Camilo José Cela S/N, 41018 Sevilla, Spain*
[b] *Center for Biomedical Research, Universidade do Algarve, Portugal*
[c] *Department of Psychology, University of Jaen, Jaen, Spain*

ARTICLE INFO

ABSTRACT

The developmental trajectories of brain oscillations during the encoding and maintenance phases of a Working Memory (WM) task were calculated. The Delayed-Match-to-Sample Test (DMTS) was applied to 239 subjects of 6–29 years, while EEG was recorded. The Event-Related Spectral Perturbation (ERSP) was obtained in the range between 1 and 25 Hz during the encoding and maintenance phases. Behavioral parameters of reaction times (RTs) and response accuracy were simultaneously recorded. The results indicate a myriad of transient and sustained bursts of oscillatory activity from low frequencies (1 Hz) to the beta range (up to 19 Hz). Beta and Low-frequency ERSP increases were prominent in the encoding phase in all age groups, while low-frequency ERSP indexed the maintenance phase only in children and adolescents, but not in late adolescents and young adults, suggesting an age-dependent neural mechanism of stimulus trace maintenance. While the latter group showed Beta and Alpha indices of anticipatory attention for the retrieval phase. Mediation analysis showed an important role of early Delta-Theta and late Alpha oscillations for mediation between age and behavioral responses performance. In conclusion, the results show a complex pattern of oscillatory bursts during the encoding and maintenance phases with a consistent pattern of developmental changes.

1. Introduction

Working memory (WM) allows encoding, maintaining, recovering, and manipulating the information for the operations necessary to solve a task (Baddeley, 2012). When the manipulative aspect is not involved and the visual modality is used, the term visual short-term memory is also employed. In the present report, we will use the term WM because, in the Delayed Match-to-Sample Test (DMTS), like the Sternberg task, selecting among possible targets or deciding whether the current stimulus was previously presented can be considered an operation; although certainly, more complex operations as in N-back tasks could add the WM updating process.

WM decays in a few seconds and has a limited storage capacity. These characteristics limit the possibilities of WM to process information. WM can hold information from several sources, such as long-term memory (LTM), newly acquired sensory information (external or interoceptive), and the products of cognitive processing, including the results

of operations performed in WM. WM enables the performance of more complex processes such as learning, language, reading, reasoning, etc. Therefore, it is necessary for daily and curricular activities. The following operational definition summarizes most of the aspects described above. "*Working memory refers to the retention of information in conscious awareness when this information is not present in the environment, to its manipulation, and to its use in guiding behavior*" (Postle, 2006).

Improvement in WM performance with age is associated with maturational brain changes. Age-related increases in structural connectivity within the frontal cortex and frontoparietal networks have been associated with age-related improvements in WM (Ostby et al., 2011; Zhou et al., 2014). Frontoparietal cortical thinning, a neural marker of brain maturation with age, is also associated with age-related WM improvement (Ostby et al., 2011). Regarding developmental changes in brain activation during WM, a *meta*-analysis comparing adolescents and young adults (Andre et al., 2015) showed increased activation of the WM network, including the left precuneus, inferior parietal
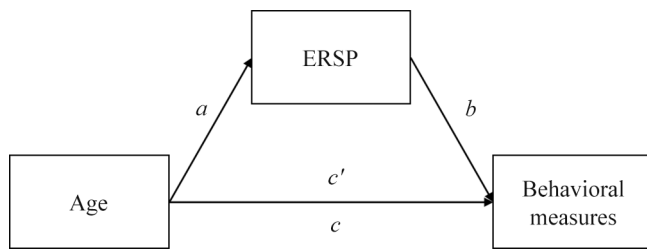
Fig. 1. Mediation model. Graphic display of the mediation model for the relationship between age and behavioral measures (RTs or correct responses) mediated by ERSP parameters.

gyri, and the middle frontal gyrus. Furthermore, decreased activation in the right superior frontal gyrus, the left junction of the inferior parietal and postcentral gyri, and the left posterior cingulate gyrus was associated with age-related increases in WM performance. A *meta*-analysis of young children has shown that activations are not only limited to frontoparietal networks but also include the insula and the cerebellum

(Yaple & Arsalidou, 2018). The role of the cerebellum in WM during development has also been demonstrated in cerebellar lesions in children (Vaquero et al., 2008).

Electroencephalography (EEG) and magnetoencephalography (MEG) allow to make inferences about the timing and anatomical location of WM subprocesses, although with low resolution due to the phenomenon of volume conduction, and can be used in children and adolescents during WM experimental paradigms such as the DMTS, Sternberg task, and N-back. In the present report, we will focus on reviewing the results of the DMTS (and the Sternberg task), since the main goal is to analyze time–frequency changes in children, adolescents, and young adults during the DMTS task.

Event-related potentials (ERPs) have been used to analyze the neurophysiology of WM development in the DMTS task. A reduction in amplitude with age has been found in visual ERPs during the encoding and retrieval phases (Barriga-Paulino et al., 2014, 2017). During the maintenance phase, a slow component appears, that has been associated with the maturation of the previously described negative slow wave (NSW) recorded during the retention phase in adults (Ruchkin et al., 1990). Neural source analysis of the NSW showed a more intense frontal
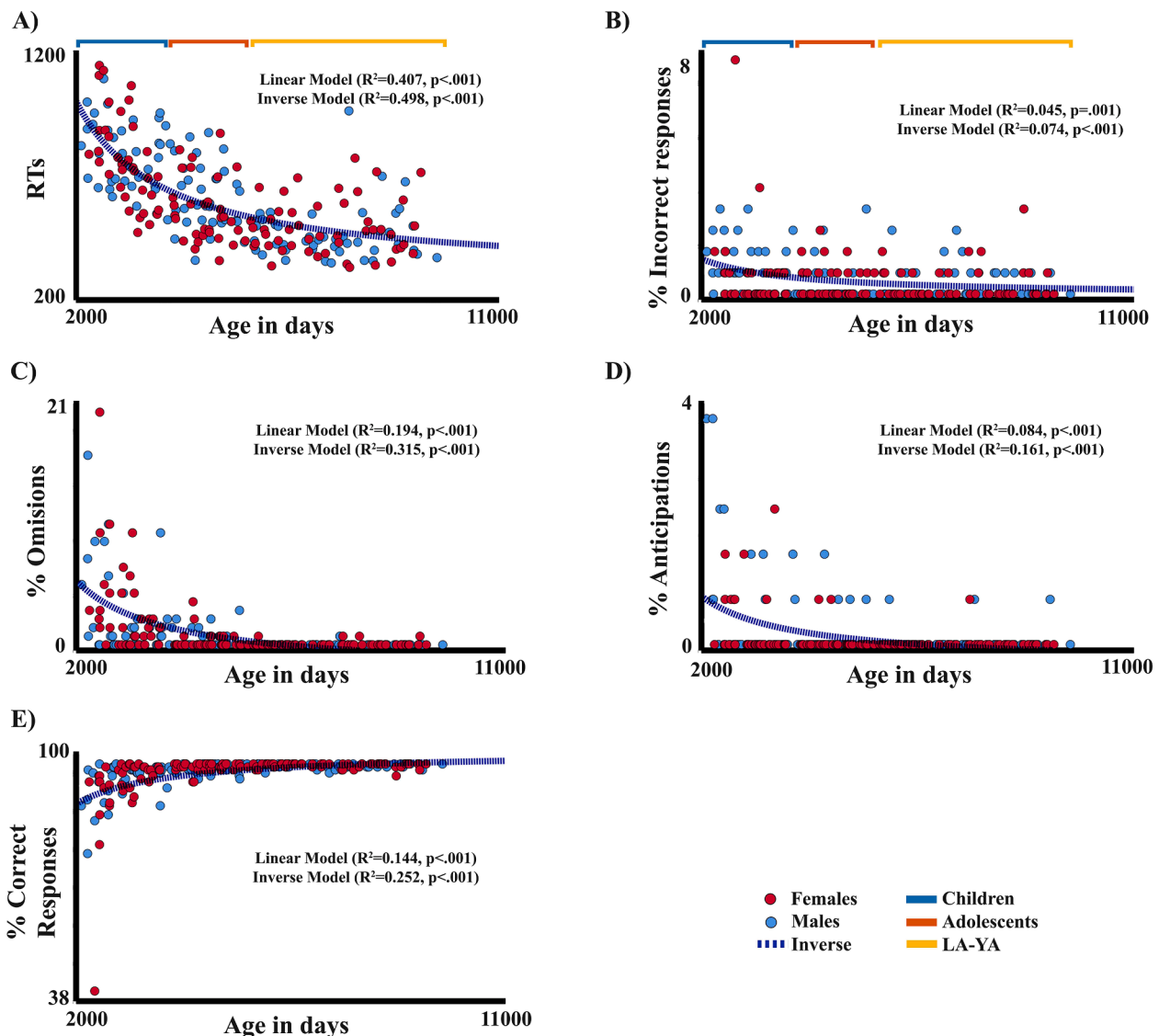
Fig. 2. Regression of behavioral parameters with respect to age. The figure displays: **2A.** Reaction Times (RTs), **2B.** Percentage of incorrect responses, **2C.** Percentage of omissions, **2D.** Percentage of anticipations, and **2E.** Percentage of correct responses linearly and inversely regressed with respect to age in days. Only the inverse regression is displayed, as it has a better fit. The subjects belonging to the different considered groups are indicated. Behavioral parameters of males and females were regressed together but displayed with a different color.

Fig. 3. ERSP absolute values during the baseline period. 3A. Display the ERSP of all subjects, ordered by age, in a color code for 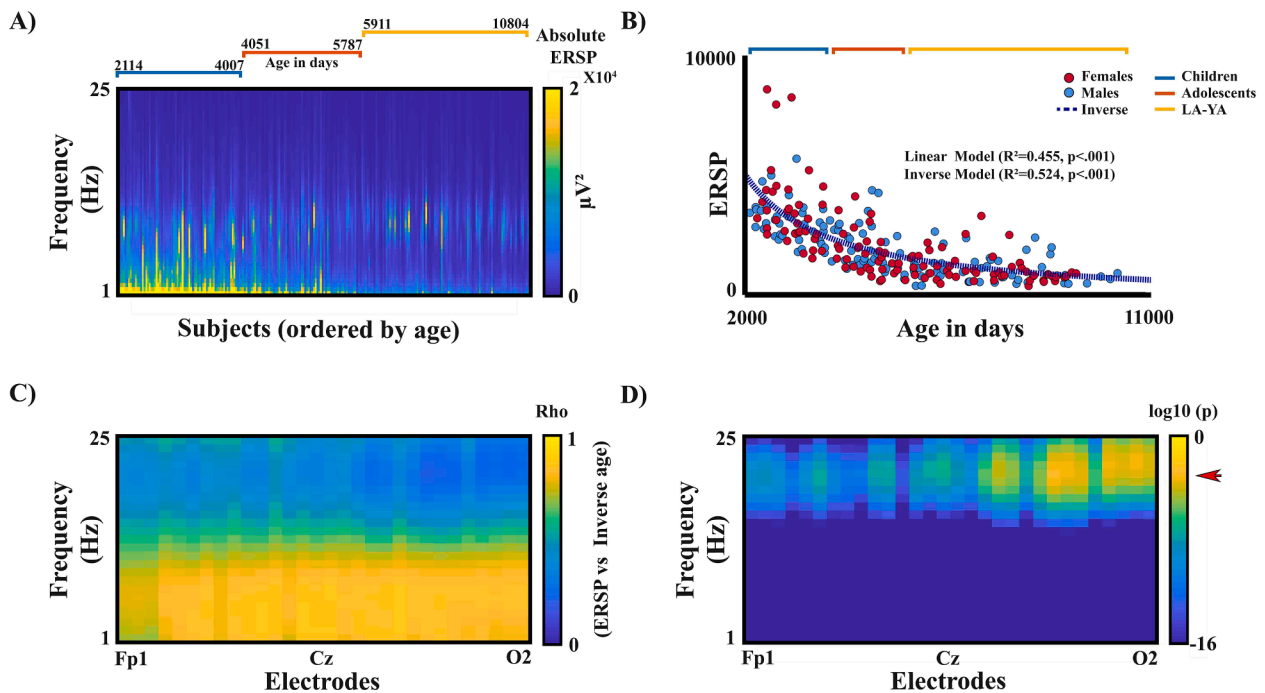the electrode Pz. **3B.** Regression of the collapse of the ERSP for all frequencies and electrodes with respect to age using linear and inverse models, only the inverse correlation is shown, as it has a better fit. **3C.** Spearman correlation values (Rho) of the ERSP values with respect to the inverse of age for all the electrodes. **3D.** Log10 (p) of the Spearman correlation showed in 3C. The arrow indicates the limit for significance level after applying the FDR correction.

neural recruitment to retain items in WM with increasing age (Barriga-Paulino et al., 2014, 2015). The reduction in ERPs with age in the DMTS WM task was also observed in N-back (Pelegrina et al., 2020) suggesting the generality of this age effect, probably due to the more general process of synaptic pruning (Huttenlocher, 1990). Indeed, an inverse relationship of age with frontal-parietal gray matter volume (a proxy for synaptic pruning) and amplitude of low-frequency EEG bands has been found (Whitford et al., 2007), suggesting that synaptic pruning should be related to a reduction in scalp EEG amplitude due to a reduction in intracerebral EEG signal generators with age. Moreover, the reduction of scalp EEG with age has been confirmed with MEG, indicating that the reduction of scalp EEG would not be related to changes in skull thickness and/or mineralization with age (Gómez et al., 2017).

Rhythmic EEG signals generated by interconnected neurons produce brain oscillations at rest or linked to stimuli or responses. The theta band has been one of the most conspicuous brain oscillations related to WM. For instance, using intracranial recordings Raghavachari et al. (2001) showed an increase in theta band Event-Related Spectral Perturbation (ERSP) during a verbal Sternberg task, including the maintenance phase. The Sternberg task is similar in some aspects to the DMTS task. One of the important mechanisms of how theta would operate in WM tasks is through theta phase coupling with gamma amplitude during the retention period of the DMTS task (Sauseng et al., 2010), whereas alpha amplitude was associated with suppression of distracting information (Sauseng et al., 2009). Indeed, brain stimulation entrainment of contralateral frontal theta and ipsilateral alpha to the target to be remembered enhances WM performance in a *retro*-cue visuospatial memory task (Riddle et al., 2020). The role of theta in WM is not only related to item retention, but also to the subsequent operation to be performed: Theta increased during the expectancy period of a cued task, where subjects have to prepare for a cued no-go, prosaccade, or antisaccade task (Cordones et al., 2013). Theta is also related to the recovery of previously presented items, with the number of theta oscillation periods during the retrieval phase being related to the number of items retained in WM (Tesche & Karhu, 2000). One of the possible roles of the

theta band in WM would be the nesting of higher frequency oscillations such as the gamma band (Buzsaki, 2006). Concerning the underlying mechanisms of WM for encoding the item trace, not only the direct effects of electrophysiological activities such as the ERPs and brain oscillations have been proposed, but also the facilitation of the synaptic pathways related to the WM processing, at least for the items outside of the attentional focus. The latter would provide a more efficient mechanism for encoding WM-related information (LaRocque et al., 2013).

Using the DMTS and Sternberg tasks, several authors have obtained evidence of neural dynamics associated with WM operation, mostly in adults and in some cases comparing controls with subjects diagnosed with several neural impairments and diseases. Koshy et al. (2020) showed a decrease in alpha and beta (8–18 Hz) during the encoding and maintenance phases of a numerical task. A similar result was obtained during encoding of an item for retention in WM, suggesting a decrease in alpha and beta Event-Related Synchronization (Zammit et al., 2018) for both, young adults and adolescents, but there were no differences between both age groups. Lenartowicz et al. (2014; 2019) using EEG in children and adolescents showed a decrease in midoccipital alpha during encoding and an increase in midfrontal theta during the maintenance phase, accompanied by an increase in alpha during the maintenance period. A result also observed by Arjona et al. (2023) in children and adolescents. The increase of alpha synchronization during the maintenance period has also been described during a DMTS task in children (Sato et al., 2018). More recently, a reduction of gamma power and gamma power variability across trials with age have also been described during the DMTS task (McKeon et al., 2023). In an object recognition task, similar to DMTS, an increase in theta and delta power and a decrease in alpha and beta power was recorded in the encoding phase (Kang et al., 2018). During the maintenance phase, a theta increase and a beta decrease were observed. Alpha/beta desynchronization was also evident in a Sternberg task, in which all items to be remembered were presented simultaneously. Interestingly, while frontal and temporal alpha/beta desynchronization was maintained up to one hundred milliseconds before retrieval, occipital alpha/beta encoding
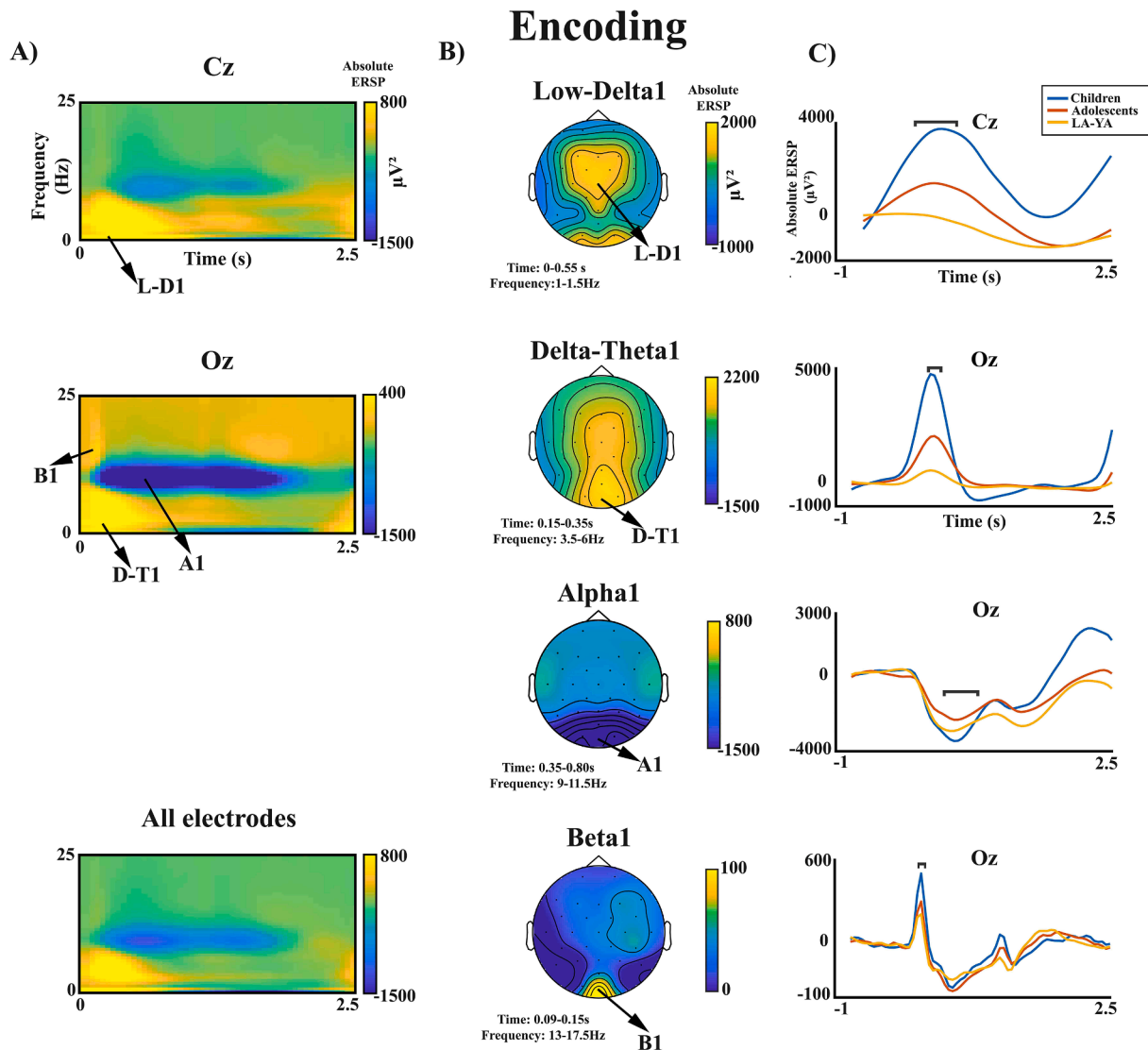
Fig. 4. **Average of Absolute Event-Related Spectral Perturbation (ERSP) panels and topography for Low-Delta1, Delta-Theta1, Alpha1, and Beta1 during the encoding phase. 4A.** Time-frequency display for 2 selected electrodes and the average of all electrodes. **4B.** Absolute ERSP topographies. The selected values for the time–frequency windows appear in the figure. The arrows in 4A and 4B indicate the time–frequency window and location of the selected time–frequency windows. **4C.** Absolute ERSP across time of the selected frequency windows for the three groups of age: children; adolescents; late adolescents and young adults. The overlying lines in 4C correspond to the ERSP time windows selected for topographies in 4B and subsequent analyses. L-D1: Low-Delta1, D-T1: Delta-Theta1, A1: Apha1, B1: Beta1, LA-YA: Late adolescents and young adults.

desynchronization became synchronized during the maintenance phase (Heinrichs-Graham & Wilson, 2015). Although an increase of theta and gamma during the delay period has generally been obtained, an increase of gamma and reduced theta in areas close to sequentially coregistered increased fMRI activity has also been reported (Khursheed et al., 2011).

Although the improvement of performance with age in the WM DMTS task is well-established, as its relationship with the NSW, the developmental trajectory of brain oscillations, and its possible relationship with WM behavioral parameters are scarcely represented in the scientific literature (reviewed in Gómez et al., 2018). Therefore, the objectives of the present report were to obtain the ERSP increases and decreases (synchronization and desynchronization, respectively), during the encoding and maintenance periods of the DMTS task, and to analyze its relationship with age and behavioral parameters. This approach would allow us to trace the developmental trajectory of transient oscillatory bursts related to the WM operation. It would be particularly important to define the electrophysiological indices of item retention in WM during the maintenance period, and its possible

relationship with age, complementing previous results obtained with ERPs. The ERSP results previously reviewed suggest a synchronization of theta accompanied by a desynchronization of alpha and beta during encoding and a return to baseline at the end of the maintenance period for alpha and beta. There is no particular hypothesis about the developmental trajectory of brain oscillations during WM operation; however, one possibility is that brain oscillations follow the well-known decrease in absolute power with age that has been described for EEG oscillatory behavior during resting state (Segalowitz et al., 2010). A relationship between brain oscillation power and behavioral responses is also expected.

2. Methods

2.1. Sample

Two hundred and fifty-one children, adolescents, and young adults participated in the study, recruited through advertisements placed in
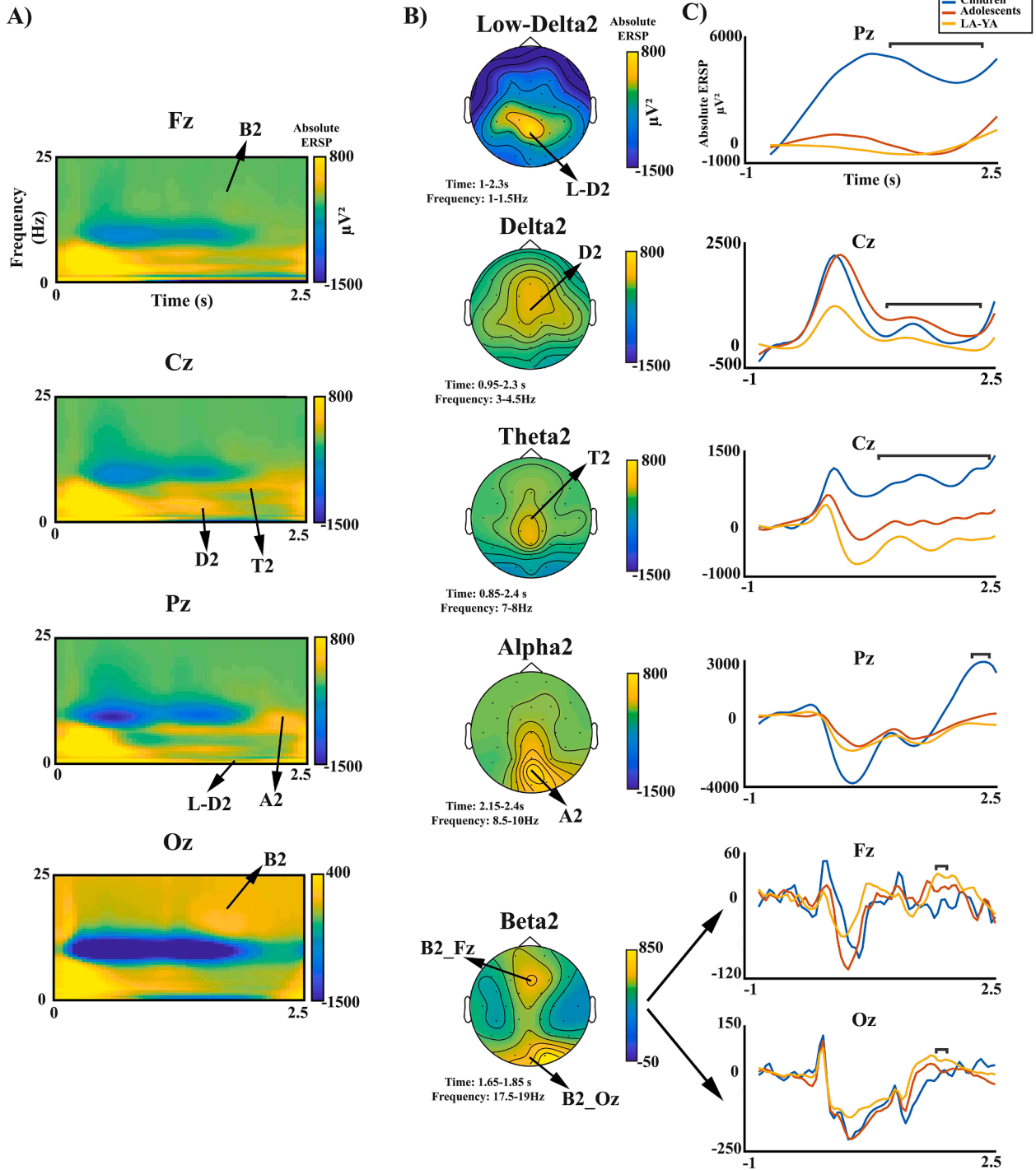
Maintenance

Fig. 5. Average of Absolute Event-Related Spectral Perturbation (ERSP) panels and topography for Low-Delta2, Delta2, Theta2, Alpha2, and Beta2. during the maintenance phase. 5A, B, and C as in Fig. 4. L-D2: Low-Delta2, D2: Delta2, T2: Theta2, A2: Alpha2, B2: Beta2, LA-YA: Late adolescents and young adults.

different schools and at the University of Sevilla. All participants reported no neurological or psychological diseases or impairments.

Subjects who did not reach a minimum of 10 artifact-free trials were eliminated from the experimental sample, resulting in a final sample of 239 (121 males/118 females, from 6 to 29 years old; mean = 14.06 years old, $SD = \pm 6.06$, with a higher number of subjects per year in children and adolescents, see Supplementary Fig. 1 for the histogram of subject's age). For some data analysis and visualization, the total sample was divided into three age groups: children (from 2114 to 4007 days of age

equivalent to 6–10 years, n = 73), adolescents (4051–5787 days equivalent to 11–15 years, n = 68) and late adolescents-young adults (LA-YA group) (5911–10804 days equivalent to 16–29 years, n = 98).

Experiments were conducted with informed and written parental consent, in accordance with the World Medical Association's Code of Ethics (Declaration of Helsinki) for experiments involving humans https://www.wma.net/en/30publications/10policies/b3/index.htm. The experimental protocol was approved by the biomedical ethical committee of the Andalucía autonomous region.

Table 1

P-*values* for the comparison with respect to baseline. The sign + or – indicates if it was higher or lower than the baseline. FDR corrected.

	p
Low-Delta1	< 0.001, +
Low-Delta2	0.052, +
Delta2	0.003, +
Delta-Theta1	< 0.001, +
Theta2	0.059, +
Alpha1	< 0.001, -
Alpha2	0.004, +
Beta1	< 0.001, +
Beta2 O2	0.059, +
Beta2 Fz	0.167, +

Table 2

P-*values* for the comparison with respect to baseline divided by age group (Children; Adolescents; Late adolescents and young adults). The sign + or – indicates if it was higher or lower than the baseline.

	P Values		
	Children	**Adolescents**	**Late adolescents and Young Adults**
Low-Delta1	< 0.001, +	0.003, +	0.045, +
Low-Delta2	0.013, +	0.819, +	0.720, -
Delta2	0.287, +	< 0.001, +	0.090, +
Delta-Theta1	< 0.001, +	< 0.001, +	< 0.001, +
Theta2	0.010, +	0.418, +	0.005, -
Alpha1	< 0.001, -	< 0.001, -	< 0.001, -
Alpha2	< 0.001, +	0.819, -	0.005, -
Beta1	< 0.001, +	0.003, +	0.946, -
Beta2 O2	0.912, -	0.819, +	< 0.001, +
Beta2 Fz	0.593, -	0.551, +	< 0.001, +

2.2. Experimental session

2.2.1. Delayed match-to-sample task

The experimental session consisted of 128 trials (see supplementary Fig. 2), organized into 4 experimental blocks, each with 32 trials. The trial started with the presentation of the first stimulus (S1), located in the center of the screen, with a visual angle of 4.56 degrees on the horizontal meridian. S1 was presented for 1000 ms and had to be memorized by the subject (encoding phase). Next, a screen with a black background and a white fixation cross in the center appeared for 1500 ms; a period during which the subject had to keep the S1 in memory (maintenance phase). Then, two stimuli (S2) appeared (one of them the same image as the S1, and the other a new stimulus), one placed on the left side and the other on the right side of the screen. S2 was presented

for 2000 ms (selection, matching, response, or retrieval phase). Retrieval will be the term used in the present report. The subject responded by pressing the left button (with his left hand) or the right button (with his right hand) of the answer box, depending on whether S2 equal to S1 appeared on the left or right side of the screen, respectively. The number of trials on each side were randomly counterbalanced. The presentation of the essays was also randomized so each subject played a different sequence. After the response, and at the end of the essay, the subject heard auditory feedback: a sound with a positive connotation if he/she hits the trial and one with a negative connotation if the response failed. Then a new trial started. Before starting the task, a practice block, consisting of 10 trials was provided to familiarize the subject with the test and ensure that the instructions were well understood. If the subject did not understand the task correctly, the practice block was repeated. The duration of the task was approximately 17 min. The S1 presentation would permit the study of encoding, the delay period for the maintenance phase and the S2 presentation would permit the study of the retrieval. The latter phase would not be studied in the present report.

2.2.2. EEG recording

EEG was recorded during the DMTS task. Subjects were instructed to look at the screen, blink as little as possible, focus on the cross presented at the center of the screen, and follow the response instructions. Recordings were obtained from 32 scalp sites using the 10–20 international system and an average reference (FP1, FPz, FP2, F7, F3, Fz, F4, F8, FC5, FC1, FC2, FC6, M1, T7, C3, Cz, C4, T8, M2, CP5, CP1, CP2, CP6, P7, P3, Pz, P4, P8, POz, O1, Oz and O2). Tin electrodes mounted on an electrode cap (ELECTROCAP) were employed. Eye movements were recorded by four electrodes: two electrodes placed at the outer canthus of each eye for horizontal movements, and two electrodes placed above and below the left eye for vertical movements. All the scalp electrodes were re-referenced off-line to the average mastoid ((M1 + M2)/2), and impedance was maintained below 10 kΩ. Data were recorded using a commercial analog–digital acquisition and analysis board (ANT) in direct current mode at 512 Hz with a 20,000 amplification gain. No filtering was applied during the recording.

2.3. Data preprocessing

EEG recordings were analyzed with EEGLAB2021.0 (Delorme & Makeig, 2004), MATLAB R2021b (MathWorks Inc., MA, USA), and FieldTrip-20210507 (Oostenveld et al., 2011). Data were filtered with a lowpass filter of 150 Hz and a high-pass filter of 0.2 Hz. The fifty Hz power line artifact was removed by employing the *pop_cleanline* function.

Eye movements, blinking, and muscle artifacts were rejected with an independent component analysis (ICA). Independent components were identified by visual inspection (Delorme et al., 2007). After EEG reconstruction, all epochs in which the EEG exceeded ± 150 µV in any

Table 3

One-way ANOVA of the ERSP in the ten selected time–frequency windows, with the age group as the between-subjects factor (df = 236), and post-hoc analysis FDR corrected. Ch: Children; Ad: Adolescents; LA-YA: Late adolescents and young adults.

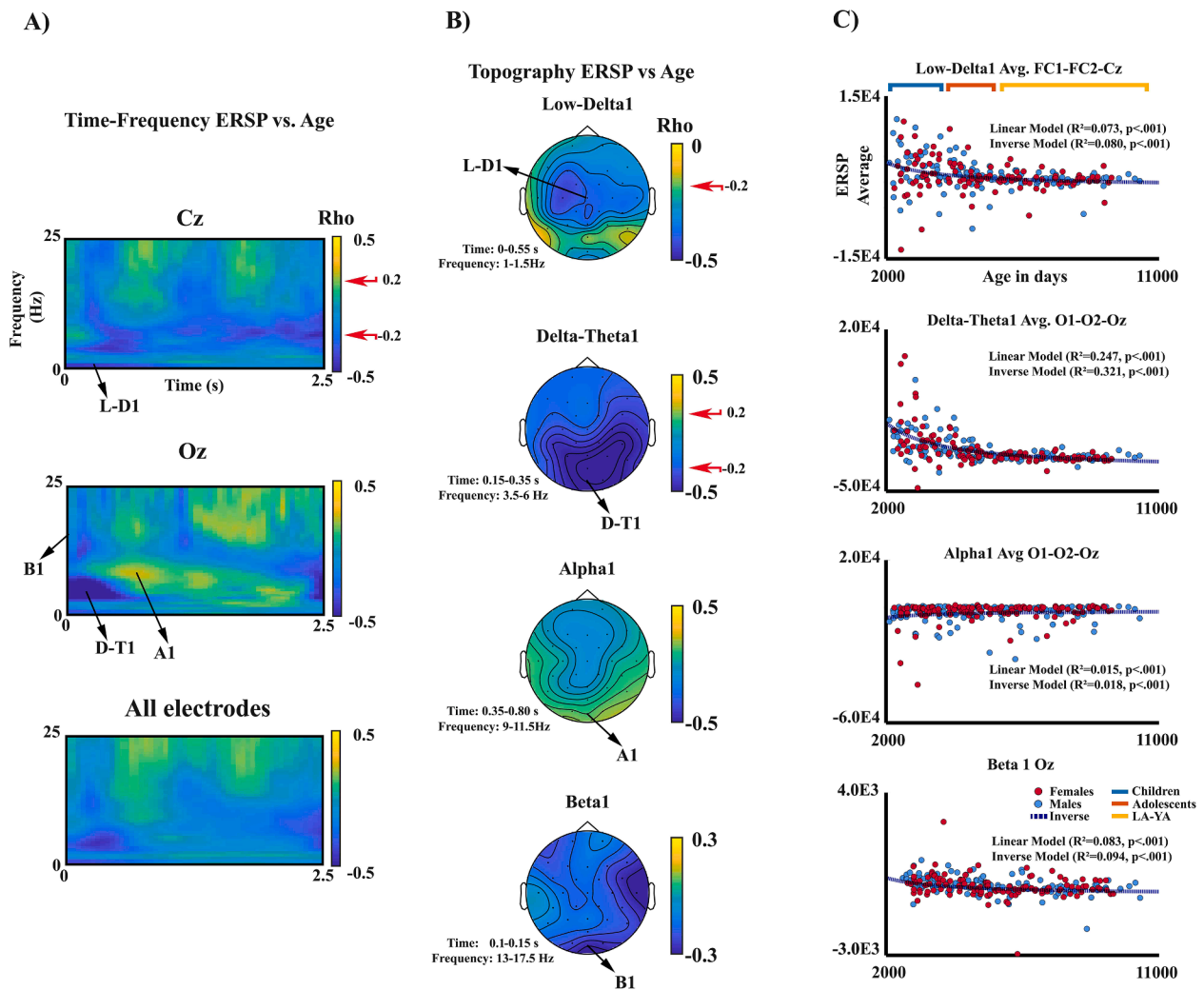|	*One-way ANOVA*		*Post-hoc*					
			Children/Adolescent		**Children/LA-YA**		**Adolescent/ LA-YA**	
	F	*p*	**< or >**	*p*	**< or >**	*p*	**< or >**	*p*
Low-Delta1	8.992	<0.001	Ch > Ad	0.002	Ch > LA-YA	<0.001	Ad > LA-YA	<0.001
Low-Delta2	5.100	0.011	Ch > Ad	0.029	Ch > LA-YA	<0.001	Ad > LA-YA	<0.001
Delta2	1.978	0.141	Ch < Ad	<0.001	Ch > LA-YA	<0.001	Ad > LA-YA	0.019
Delta-Theta1	42.461	<0.001	Ch > Ad	<0.001	Ch > LA-YA	<0.001	Ad > LA-YA	<0.001
Theta2	9.995	<0.001	Ch > Ad	0.029	Ch > LA-YA	0.007	Ad > LA-YA	0.948
Alpha1	2.195	0.126	Ch < Ad	0.035	Ch < LA-YA	0.122	Ad > LA-YA	0.421
Alpha2	31.046	<0.001	Ch > Ad	<0.001	Ch > LA-YA	<0.001	Ad > LA-YA	0.980
Beta1	13.937	<0.001	Ch > Ad	0.070	Ch > LA-YA	0.184	Ad > LA-YA	0.929
Beta2 O2	2.499	0.105	Ch < Ad	0.597	Ch < LA-YA	0.002	Ad < LA-YA	0.018
Beta2 Fz	2.550	0.105	Ch < Ad	0.029	Ch < LA-YA	<0.001	Ad < LA-YA	0.088

Fig. 6. ERSP amplitude relationship with age during the encoding phase. 6A. Spearman correlation (Rho) of ERSP vs. age panels for selected electrodes and collapsing all electrodes (below). The arrows in the color bar indicate the limits for Rho significance after applying the False Discovery Rate **6B**. Topographies of the ERSP vs. age Spearman correlation averaging the time–frequency windows indicated. The arrows from 6A to 6B indicate the corresponding region in the time-–frequency plots. **6C.** Linear and inverse regressions of the ERSP with age, collapsing the correlation values in the electrodes and time–frequency windows indicated in Fig. 6B. Only the correlation with the better fit is displayed. L-D1: Low-Delta1, D-T1: Delta-Theta1, A1: Apha1, B1: Beta1, LA-YA: Late adolescents and young adults.

channel were discarded. As indicated previously, only the 239 subjects who had a minimum of 10 correct trials were analyzed.

3. Data analysis

3.1. Event related Spectral Perturbation (ERSP)

Time-frequency analysis allows observation of dynamic changes in spectral power, measured as ERSP relative to baseline, and phase. In the present report, we will focus on ERSP after subtracting the ERSP value from the baseline power. Note that although other studies have used different types of relative measures (Cohen, 2014), in the present report we preferred to use absolute values to consider the possible high dependence of ERSP with age. To study the time–frequency behavior of the electrical activity elicited by the stimuli presented in the trial, single trials (from 1 s before S1 to 7 s after S1) were convolved with a complex Morlet wavelet, using a 7 cycles wavelet, through the *ft_freqanalysis* function of FieldTrip (Oostenveld et al., 2011). ERSP values were maintained as absolute values, as the main interest was to observe changes in ERSP across ages. The baseline was applied in the period −800 ms to −400 ms before S1, to minimize the overlap of slow

frequencies between the baseline and the perturbations induced by the stimulus. The frequency range analyzed was 1–25 Hz. High-frequency analysis (>25 Hz) was avoided due to the described contamination of these frequency ranges by muscle artifacts (Goncharova et al., 2003). ERSP values were averaged across trials. To observe which frequency oscillations are the most important for each of the WM subprocesses, the average of all the subjects was computed. This procedure allows to eliminate any bias due to age in the selection of frequencies and time windows for further analysis.

3.2. Behavioral statistical analysis

The developmental trajectories of Reaction Times (RTs) and the percentage of incorrect responses, anticipations, and omissions were obtained. Non-responses to S2 were considered omissions; responses on the side of the novel stimulus were considered incorrect responses, and the responses to S1 during the maintenance period or responses faster than 200 ms after S2 were considered anticipations. These behavioral parameters were linearly regressed vs age expressed in days. The inverse model, as an alternative model, was computed by regressing the behavioral parameters vs. the inverse of age. To correlate the behavioral
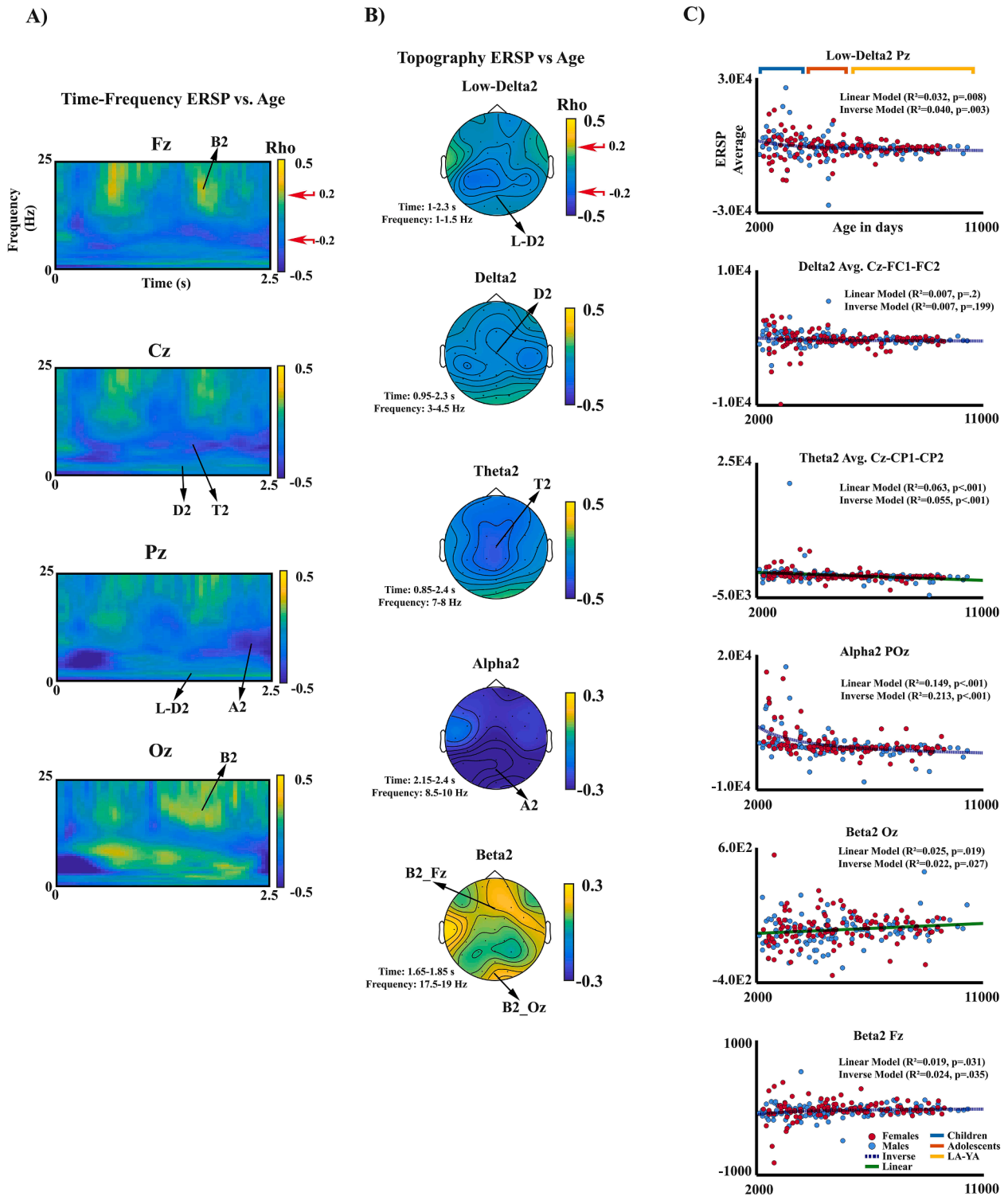
Fig. 7. ERSP amplitude relationship with age during the maintenance phase. 7A, B, and C as in Fig. 6. L-D2: Low-Delta2, D2: Delta2, T2: Theta2, A2: Alpha2, B2: Beta2, LA-YA: Late adolescents and young adults.

parameters with the ERSP, and to reduce dimensionality, the percentage of correct responses was also computed by excluding all error types. The effect of gender on the behavioral parameters was analyzed by t-tests comparing both groups. No significant differences were found in any of the gender comparisons; therefore, gender was excluded from further behavioral analyses.

3.3. ERSP analysis

ERSP were analyzed in absolute values in two different analysis periods: baseline and post-S1 (encoding and maintenance periods). ERSP during baseline (-.8s to -.4s) were used to obtain the EEG spectral composition during baseline (time–frequency panels). These values were regressed against the inverse of age. Additionally, mean ERSP values were collapsed across frequencies and electrodes during the

Table 4

P-*values* of the FDR corrected Spearman correlations between ERSP amplitudes
with Rts and the percentage of correct responses.

ERSP	Rts		%Correct Responses	
	Rho	*p*	Rho	*p*
Low-Delta1	0.186	0.010	-0.164	0.020
Low-Delta2	0.078	0.235	-0.170	0.019
Delta2	0.202	0.005	-0.125	0.072
Delta-Theta1	0.478	< 0.001	-0.330	< 0.001
Theta2	0.338	< 0.001	-0.163	0.020
Alpha1	-0.111	0.103	0.136	0.051
Alpha2	0.460	< 0.001	-0.307	< 0.001
Beta1	0.273	< 0.001	-0.156	0.025
Beta2 O2	-0.105	0.118	0.208	0.004
Beta2 Fz	-0.118	0.086	0.164	0.020

baseline period and correlated with the inverse of age. The latter approach allowed us to observe the age dependence of brain rhythms not yet engaged in the task.

The use of time–frequency windows, in a non-biased manner, rather than continuous statistical testing such as the cluster-mass approach (Maris & Oostenveld, 2007; Oostenveld et al., 2011) across the whole time–frequency and electrode space, was preferred for ERSP analysis to reduce the dimensionality of the data, which would make the statistical power of the analysis difficult given the high data dimensionality in terms of frequencies, periods, and electrodes.

Averaging across the 239 subjects of the time–frequency panels of the absolute ERSP values produced a landscape of the oscillatory response to S1 presentation across electrodes during the encoding and maintenance periods. Some time–frequency intervals showed increments or decrements of ERSP amplitude, with respect to baseline, after the S1 presentation, including the encoding and maintenance phases. By averaging all subjects across ages, it was possible to obtain ERSP time–frequency panels that were not biased by age. To capture the electrodes where these dynamic responses occurred, the ERSP in the selected time–frequency windows were plotted topographically using the *EEGLAB topoplot* function. These latter procedures allowed the extraction of the electrodes, time windows, and frequencies in which the responses to S1 were more evident during the encoding and maintenance periods. The following criteria were used to select time–frequency

windows and electrodes for further analysis: (i) the p-value should be significant compared to the baseline in at least one of the age groups, (ii) the time window should be centered around the peak amplitude of the selected frequency, (iii) the selected electrodes should present the maximum amplitude when topographically represented. Note also that the fact of selecting the time–frequency windows by the around peak activity criterion is completely unbiased with respect to the age group comparison since these features are selected in the collapsed across ages. The selected time–frequency windows were named as LowDelta1 (electrodes: FC1, FC2, Cz; time window: 0–0.55 s, frequency window: 1–1.5 Hz), LowDelta2 (Pz; 1–2.3 s; 1–1.5 Hz), Delta2 (FC1, FC2, Cz; 0.95–2.3 s; 3–4.5 Hz), Delta-Theta1 (O1, O2,Oz; 0.15–0.35 s; 3.5–6 Hz), Theta2 (Cz, Cp1, Cp2; 0.85–2.4 s; 7–8 Hz), Alpha1 (O1, O2, Oz; 0.35–0.80 s; 9–11.5 Hz), Alpha2 (POz; 2.15–2.4 s; 8.5–10 Hz), Beta1 (Oz, 0.1–0.15 s; 15–17.5 Hz); and Beta2, extracted independently in two different electrodes (O2 and Fz; 1.65–1.85 s; 17.5–19 Hz). Note that the strategy used to extract the time and frequency windows defined for further analysis is not biased because it is based on the average of all subjects. Similarly, the selection of electrodes for statistical analysis was based on the topography of the whole sample. Therefore, any age-related results cannot be attributed to a posteriori selection of electrodes or time and frequency windows.

The effect of gender on the ten ERSP time and frequency windows described in the preceding paragraphs was analyzed by t-tests comparing males and females. No significant differences were found in any of the gender comparisons; therefore, gender was excluded from further behavioral analyses. To test if the visually selected time and frequency windows were significantly different from the baseline, a *t*-test was applied to the mean ERSP values across the selected electrodes of each selected time–frequency window. Baseline comparisons were also computed for each of the selected time–frequency windows for the three age groups (children, adolescents, and LA-YA). A one-way ANOVA with age as the between-group factor was computed for the ERSP in each time–frequency period. To have a more continuous definition of the relationship between ERSP and age, a regression approach was used to characterize the developmental trajectories, instead of the more classical post-hoc comparisons. Mean values of each of these time–frequency periods across the selected electrodes were obtained and regressed linearly and inversely to age. The regression was complementary to ANOVAs to assess the effect of age on ERSP and was used in addition to

Table 5

Mediational analysis. Standardized direct and indirect effects of age through ERSP amplitudes on behavioral measures.

Outcome	ERSP Mediator	a	b	a × b	95% CI	c'	c
Response Time							-0.641**
	Low-Delta1	-0.269**	0.023	-0.006	[-0.034, 0.022]	-0.635**	
	Low-Delta2	-0.171*	-0.044	0.007	[-0.011, 0.026]	-0.649**	
	Delta2	-0.074	-0.010	0.001	[-0.007, 0.008]	-0.642**	
	Delta-Theta1	-0.499**	0.162*	-0.081*	[-0.140, -0.022]	-0.561**	
	Theta2	-0.337**	0.035	-0.012	[-0.048, 0.024]	-0.629**	
	Alpha1	0.125	0.058	0.007	[-0.007, 0.022]	-0.649**	
	Alpha2	-0.382**	0.177*	-0.067*	[-0.113, -0.022]	-0.574**	
	Beta1	-0.282**	0.058	-0.016	[-0.046, 0.014]	-0.625**	
	Beta2 O2	0.135	0.021	0.003	[-0.011, 0.017]	-0.644**	
	Beta2 Fz	0.135	-0.064	-0.009	[-0.024, 0.007]	-0.633**	
Correct Responses							0.379**
	Low-Delta1	-0.269**	-0.033	0.009	[-0.025, 0.042]	0.370**	
	Low-Delta2	-0.171*	-0.046	0.008	[-0.014, 0.029]	0.371**	
	Delta2	-0.074	-0.111	0.008	[-0.009, 0.025]	0.371**	
	Delta-Theta1	-0.499**	-0.080	0.040	[-0.029, 0.109]	0.339**	
	Theta2	-0.337**	-0.060	0.020	[-0.023, 0.064]	0.359**	
	Alpha1	0.125	0.075	0.009	[-0.008, 0.027]	0.370**	
	Alpha2	-0.382**	-0.376**	0.144**	[0.080, 0.208]	0.235**	
	Beta1	-0.282**	-0.010	0.003	[-0.032, 0.038]	0.376**	
	Beta2 O2	0.135	0.032	0.004	[-0.012, 0.021]	0.375**	
	Beta2 Fz	0.135	0.115	0.016	[-0.006, 0.038]	0.363**	

Note: ** p <.001, * p <.05; p-values were adjusted using FDR; *a*: coefficients for the path from age to ERSP measures; *b*: coefficients for the path from ERSP amplitudes to behavioral measures (Rts and correct responses); *a* × *b*: indirect effects of age on behavioral measures through ERSP amplitudes; *c'*: direct effects of age on behavioral measures; *c*: total effects of age on behavioral measures; CI: confidence interval for the coefficients *a* × *b*.

post-hoc comparisons because regression analysis allows obtaining a continuous developmental trajectory without imposing arbitrary age limits on the age groups.

3.4. Relationship between ERSP and behavior

To observe possible correlations between ERSP and behavioral parameters Spearman correlations were calculated between the RTs and the percentage of correct responses with the ERSP values collapsed across the selected electrodes in the 10 defined time–frequency windows. Since no gender differences were found for the behavioral and ERSP parameters, all subsequent regression and correlation analyses were performed regardless of gender. All p-values shown in the present report were adjusted using the Benjamini & Hochberg (1995) false discovery rate (FDR). The FDR was calculated using the FDR_bh function from the Mass Univariate ERP Toolbox (Groppe et al., 2011). The implementation of the FDR in each dataset can be found in the supplementary methodological material.

In addition, to determine the possible mediating role of ERSP parameters in the relationship between age and behavioral measures, a series of mediation analyses were conducted. The general model is shown in Fig. 1. The term *a* refers to the coefficient for the path from age to the mediator variables (i.e., ERSP parameters). The term *b* indicates the path from the mediators to the behavioral measures: RTs and correct responses. The term $a \times b$ quantifies the indirect effect of age on behavioral measures through the ERSP mediators. The total effect *c* is the relationship between age and behavioral measures. The direct effect *c'* quantifies the effect of age on behavioral measures that is independent of the indirect effects. Therefore, *c'* is equivalent to subtracting the indirect effect from the total effect of age on behavioral measures. All included variables were standardized to ensure that they were on the same scale. Mediation analyses were performed using the lavaan package (Rosseel, 2012) in R (version 4.2.0; R Core Team, 2020).

4. Results

4.1. Behavioral results

RTs and the percentage of incorrect responses, omissions, anticipations, and total correct responses (Fig. 2) showed an improvement with age that was modeled better by an inverse relationship with age than by a linear relationship with age (RTs (Linear model ($R^2 = 0.407$, p <.001), Inverse model ($R^2 = 0.498$, p <.001)); % Incorrect responses (Linear model ($R^2 = 0.045$, p <.001), Inverse model ($R^2 = 0.074$, p <.001)); % Omissions (Linear model ($R^2 = 0.194$, p <.001), Inverse model ($R^2 = 0.315$, p <.001)); %Anticipations (Linear model ($R^2 = 0.084$, p <.001), Inverse model ($R^2 = 0.161$, p <.001)); % Correct responses (Linear model ($R^2 = 0.144$, p <.001), Inverse model ($R^2 = 0.252$, p <.001))).

4.2. Event Related Spectral Perturbtion (ERSP) vs. age during baseline

The ERSP during the baseline period (Fig. 3) showed the typical spectral pattern of 1/frequency decrease with age accompanied by an Alpha rebound (Fig. 3A). To quantify the ERSP decrease with age during the baseline period, the ERSP was collapsed across electrodes and frequencies. The collapsed ERSP was significantly related to age for both: negatively linear and inverse regression models (Fig. 3B) (Linear model ($R^2 = 0.455$, p <.001); Inverse Model ($R^2 = 0.524$, p <.001)). Correlation of absolute ERSP with the inverse of age during baseline showed a significant decrease in power at all electrodes, with a higher correlation at low frequencies and in the Beta band, and a lower correlation in the Alpha band (Fig. 3C). All correlations were significant after adjustment for FDR (Fig. 3D).

4.3. Event Related Spectral Perturbation (ERSP) vs. age during encoding and maintenance

The ERSP after the presentation of S1, including encoding and maintenance periods, showed a complex response with several amplitude increases or decreases when compared to the baseline (Figs. 4 and 5). Fig. 4A and 5A show the time–frequency plot for selected electrodes and the time–frequency collapse for all electrodes and subjects. Several ERSP increases and decreases are shown. The topographies and the time dynamics at selected frequencies across time are shown in Fig. 4B, 5B, 4C, and 5C. Arrows in the figures indicate the location of the selected time–frequency windows used for the displayed topographies. These amplitude changes in ERSP relative to baseline were identified as Low-Delta1 (central and posterior distribution during the encoding period), Low-Delta2 (parietal during maintenance phase), Delta2 (fronto-central during maintenance), Delta-Theta1 (posterior during encoding), Theta2 (centro-parietal during maintenance), Alpha1 (posterior during encoding and maintenance periods), Alpha2 (posterior during maintenance), Beta1 (posterior during encoding) and Beta2 (anterior and posterior during maintenance phase).

FDR corrected t-tests of ERSP amplitude compared to baseline showed that most of the visually selected time–frequency windows were significant (Table 1), except for Low-Delta2 Theta2, and Beta2 (O2), which showed a trend for significance, and Beta2 (Fz), which was not significant. The results of the t-tests computation with respect to baseline independently for the three age groups are shown in Table 2. These latter analyses (Tables 1 and 2) confirmed that were significant results when compared to the baseline for all selected time–frequency windows and that there was a strong age dependence for the ERSP. Only the ERSP amplitude of Low-Delta1, Delta-Theta1, and Alpha1 were significant compared to the baseline for all three age periods. Fig. 4C and 5C and Table 2 show that in most cases there was a decrease in ERSP amplitude with age for all frequency ranges except for three cases. Alpha1 in which there was an increase, since Alpha1 corresponds to a decrease in the alpha range with respect to baseline, it is in a sense also a decrease in amplitude with age. Beta2 in anterior (Fz) and posterior (O2) electrodes showed a power increase with age.

The strong dependence of ERSP with age was confirmed by the one-way ANOVA with the age group as a between-subject factor (Table 3). Table 3 shows the FDR p-adjusted values showing a significant age effect for most time–frequency windows except for Delta2, Alpha1, and Beta2 (in anterior and posterior locations). The time windows used for the ANOVA are shown in Fig. 4C and 5C, which also show trends for an increase or decrease in ERSP with age. As indicated in the methods section, in addition of post-hoc t-test comparisons (displayed in Table 3), Spearman correlation of ERSP vs age and ERSP developmental trajectories using linear and inverse models were preferred to obtain a continuous picture of ERSP developmental changes. To quantify the age dependence of ERSP values, Spearman correlations were performed between ERSP values and age. Fig. 6A and 7A show the Spearman correlations between ERSP and age. The correlations show that the selected time–frequency shows a predominantly negative relationship, except for Alpha1, in posterior sites and Beta2 in anterior and posterior sites in which a positive relationship with age was found. Fig. 6B and 7B show the topographies of Spearman correlations vs. age in the 10 selected time–frequency windows during the encoding and maintenance phases. The correlation maps show ERSP peaks with high age correlation roughly similar to the electrodes where ERSP showed higher amplitude, with Alpha1 and Beta2 being the only ones that showed positive correlations. Fig. 6C and 7C show the linear and inverse regression of ERSP with respect to age in the electrodes proposed in Figs. 4 and 5 as the electrodes of maximum activity for a given ERSP time–frequency window. These relationships were significant for most comparisons, except for Delta2. The inverse age model showed a higher explained variance than the linear age model in most cases. Figs. 6B and 7B show the topographies of the Spearman correlation of the selected ERSP

time–frequency windows amplitude with age.

Additionally, and to prove that the ERSP amplitudes are constant across the broad age distribution in the LA-YA group, FDR corrected t-tests were computed for the ERSP amplitude of the 16–20 and 21–29 year age subgroups, for the ten selected time–frequency windows. The FDR-corrected p-values (Supplementary Table 1) indicated no significant differences between ERSP amplitudes in these two age subgroups in the LA-YA age range.

4.4. ERSP vs behavioral parameters correlation

The ERSP amplitude of the different brain oscillations analyzed was correlated with the RTS and the percentage of correct responses. Table 4 shows the Spearman correlation values (FDR corrected) of the 10 measures of ERSP amplitudes with the RTs and the percentage of correct responses. Most of the correlations were statistically significant. When partial correlations were computed controlling for the inverse of age, only the FDR corrected partial correlation between correct responses and Alpha2 remained significant (responses (Rho = -0.304, p <.001).

4.5. ERSP mediation between age and behavioral performance

The results of the mediation models for age as a predictor are shown in Table 5. Age was a significant predictor of RT and correct responses (c = -0.64 and c = 0.38, respectively). The effects of age on the behavioral variables were partially mediated (coefficients $a \times b$) through ERSP Delta-Theta1 (RTs), and Alpha2 (RTs and correct responses). The effect of age decreased but did not disappear (coefficient c') when the mediation of Alpha2 and Delta-Theta1 was taken into account.

5. Discussion

The present recording and analyses have allowed us to obtain the synchronization and desynchronization that appears embedded in the EEG related to the encoding and maintenance periods of the DMTS task during development. The results indicate a myriad of transient and sustained bursts from low frequencies (1 Hz) to frequencies in the beta range (up to 19 Hz). These oscillatory bursts and sustained activities of brain oscillations showed defined topographies and were age-related, in most cases showing a decrease in amplitude with age, similar to the decrease in power with age observed in resting-state EEG oscillations. ERSP comparisons with the baseline of the selected unbiased time–frequency windows showed that they were significantly different from the baseline when considered in the total sample or when considered in different age groups, validating the psychophysiological relevance of the selected time–frequency windows. The amplitude of brain rhythms changed during the encoding and maintenance periods and correlated with behavioral responses but in an age-dependent manner. Early Delta and Theta (Delta-Theta1) and late Alpha (Alpha2) were the brain rhythms more related to behavior. We discuss the dynamics and possible psychophysiological role of these WM responsive oscillations. Interestingly, no gender differences were found in oscillatory bursts associated to WM processing, while in other types of tasks, such as speech perception, gender EEG oscillatory differences were found related to forward models of speech perception (mu-beta rhythm higher desynchronization in males) and sensorimotor inhibition (mu-alpha rhythm higher synchronization in females) (Thornton et al., 2019; Jenson et al, 2020). The different nature of the tasks, WM, and speech perception would justify the obtained differences.

As a control analysis, power was computed in the baseline period to confirm the standard behavior of the developmental trajectories of EEG in the present sample. The results indicated that for all frequencies and electrodes analyzed, there was an inverse relationship of power with age, as it has been obtained in previous reports during the resting state (Segalowitz et al., 2010; Lüchinger et al., 2011; Rodríguez-Martinez et al., 2012).

The initial response to the encoded stimuli consisted of a posterior Delta-Theta activity (labeled as Low_Delta1 and Delta-Theta1), a very short Beta response (Beta1), and a long Alpha1 decrease that lasted until the maintenance phase, all with a posterior topography. Compared with baseline ERSP Delta-Theta1 and Beta1 activity were significant (ERSP > baseline) in all three age groups, except for Beta1 in the LA-YA group, indicating the high robustness of these responses. The Delta-Theta response possibly corresponds in large part to visual event-related potentials (VERPs), a classic response that has been recorded in a variety of visual stimulation experimental paradigms (Hillyard & Anllo-Vento, 1998). The relationship of VERPs such as P3 and N2 to slow frequency components has been broadly described (Harper et al., 2014; Bachman & Bernat, 2018). The obtained inverse relationship of Delta-Theta1 power with age is similar to that obtained in DMTS and N-back VERPs (including C1, P1, P2, N2, P3, and late positive component), which also showed the inverse relationship with age obtained in the present report (Barriga-Paulino et al., 2017, Pelegrina et al., 2020). Simultaneously to the Delta-Theta activity, an occipital Beta burst (Beta1) emerged from a very narrow temporal window; the frequency 13–17 Hz content of this Beta burst implies oscillatory periods of 58–77 ms, suggesting that it could also be part of the VERPs, since the duration of the C1, P1, and N1 VERPS are in this duration range. Beta responses were significantly inversely related to age, similar to the inverse relationship with age of the C1, P1, and N1 VERPs (Barriga-Paulino et al., 2017). The most plausible explanation for this age-related decrease in ERSP amplitude would be cortical pruning (Huttenlocher, 1990, Whitford et al., 2007). Given the similar time window, frequency content, and topography of early Delta-Theta and Beta responses with VERPs, their role in processing visual stimulus properties can be suggested, as has been widely described for visual evoked potentials (Hillyard & Anllo-Vento, 1998), with a subsidiary function in S1 stimulus encoding for the proposed WM task. From a behavioral functional point of view, a correlation between the power of brain oscillations during the encoding phase and behavioral responses was expected and obtained, given the similar developmental trajectory of both during the encoding phase: brain oscillations and behavioral responses (RTs and correct responses). However, only Delta-Theta1 mediated the relationship between age and RTs, and no mediation effect of ERSP was found for the relationship between age and correct responses. Delta-Theta oscillations are related to late VERPS positivities, including P300. The P300 has been linked to the attentional capacity and facilitates the encoding of information into memory (Polich, 2007). Delta-Theta mediation between age and RTs would be related to the increased attentional capacity for task engagement that occurs as age increases, a process that has been linked to P300 maturation, which is related to increases in processing speed (Pelegrina et al., 2020).

During the maintenance period, four ERSP activities were obtained showing traces of activity, the so-termed as Low-Delta2, Delta2, Theta2, and Alpha1. The latter was already present in the encoding phase and propagate to the maintenance period. When ERSPs were compared with baseline, Low-Delta2 was significant only in children (ERSP > baseline), Delta2 only in adolescents (ERSP > baseline), Alpha1 in all three age groups (ERSP < baseline), and Theta2 was significant in children (ERSP > baseline) and LA-YA (ERSP < baseline). Therefore, the maintenance phase results, show that low-frequency ERSP increases occur when the stimulus trace must be kept in WM in children and adolescents. The latter process would be facilitated by the reduction of Alpha obtained during encoding and maintenance phases. The ERSP decrease in Alpha and Beta frequencies during the maintenance period has been widely described as a possible mechanism for facilitating the carrier of the WM trace (Raghavachari et al., 2001; Cordones et al., 2013; Lenartowicz et al., 2014; Heinrichs-Graham & Wilson, 2015; Kang et al., 2018; Koshy et al., 2020). This result is consistent with the general finding that alpha desynchronization would be related to a state of cortical activation, as proposed in the gating by inhibition (GBI) hypothesis (Klimesch, 2012; Jensen and Mazaheri, 2010. The dependence of alpha amplitude with

age (both: Alpha1 and Alpha2), supports a possible role of cortical activation-inhibition by alpha for the behavioral performance in the DMTS task. Alpha desynchronization, which can also be observed during the encoding phase, can be extended from the present results to children and adolescents. In a small number of reports, increases in low-frequency ERSP accompanies Alpha and Beta desynchronization, being a potential information carrier for WM trace (Raghavachari et al., 2001; Cordones et al., 2013; Lenartowicz et al., 2014; Kang et al., 2018). However, in the present report, increases in low frequency (Low-Delta2, Delta2, and Theta 2) were found in children and/or adolescents, but not in the LA-YA group. The difference with other reports that have found such an increase could be due to the type of experimental paradigms. However, the latter result leaves open the question of what mechanism would be involved in keeping the stimulus trace in WM during the maintenance period in young adults and late adolescents. Two possible mechanisms, not explored in the present report, are the phase-amplitude coupling between low and high-frequency signals (Sauseng et al., 2009, 2010), and synaptic weight modification during memory tasks (LaRocque et al., 2013). While most of these oscillatory activities were related to behavioral responses, they did not produce a mediation between age and behavioral responses.

At the end of the maintenance period, posterior Alpha2 and anterior-posterior Beta2 were evident. Alpha2 was statistically significant compared to baseline at the end of the maintenance period only in the LA-YA group, presenting Alpha2 a significant effect of the age factor with a developmental trajectory of decreasing power with age. A similar Alpha synchronization has been found in posterior areas during the maintenance phase (Lenartowicz et al., 2014, 2019), and at the end of this phase (Heinrichs-Graham & Wilson, 2015). In the present report, it was only in the last few hundred milliseconds before the end of the maintenance phase, probably due to the shorter duration of this phase. Alpha synchronization during this phase has been attributed to reflect inhibition of the visual cortices to facilitate the gating of the incoming stimuli (Lenartowicz et al., 2014; Heinrichs-Graham & Wilson, 2015). This functional interpretation is supported by the mediation produced by Alpha2 on the relationship between age with RTs and correct responses. The small, but significant increase compared to the baseline of Beta2 in anterior and posterior sites, only in the LA-YA group, can be interpreted as anticipatory attention for action (frontal sites) and perception (posterior sites) during retrieval. This suggestion is supported by the well-known role of Beta synchronization in attention (Vázquez-Marrufo et al., 2001). The fact that children and adolescents showed only a return to baseline levels of Alpha2 and no increase in Beta2 suggests a reduced capacity for anticipatory attention, which is reflected behaviorally in worse WM performance.

In conclusion, the results show the presence of a complex pattern of oscillatory bursts during the encoding and maintenance phases with a consistent pattern of developmental change. The behavioral relationship between the maturation of the oscillatory activity was significant for RTs and the response accuracy, however, when testing for the mediation of oscillatory activity between age and behavior, only the Delta-Theta1 and Alpha2 were significant, suggesting a role of attentional engagement and focusing for WM improvement with age in the DSTM task. The results suggest that the presence of Beta and low-frequency components are crucial for encoding the S1 stimulus, while Alpha would allow the sharpening of this process. Interestingly, the results suggest that it is possible that in adults there is a limited role of low-frequency increase in keeping the WM trace active, at least in WM tasks related to visual short-term memory such as DMTS, while in children and adolescents, the low-frequency component would play an important role. Conversely, anticipatory attention previous to the retrieval phase would be characterized by an increase in Alpha and Beta in late adolescents and adults. In fact, Alpha2 has shown the most consistent relationship with the behavioral responses of the 10 brain oscillations analyzed.

One limitation of the present report lies in the very limited number of incorrect responses, which precluded the possibility of comparing correct and incorrect responses, which would have allowed us to obtain a better understanding of the functional value of each of the oscillatory bursts described here. Another limitation arises from the difficulty to disambiguate pure WM processes from attentional processes, in part due to the close relationship between WM and attentional operations.

Data availability

Data are available under reasonable request to the corresponding author (cgomez@us.es).

CRediT authorship contribution statement

Carlos M. Gómez: Conceptualization, Formal analysis, Methodology, Funding acquisition, Project administration. **Vanesa Muñoz:** Writing – review & editing, Visualization. **Elena I. Rodríguez-Martínez:** Software, Investigation. **Antonio Arjona:** Software, Investigation. **Catarina I. Barriga-Paulino:** Software, Investigation. **Santiago Pelegrina:** Formal analysis, Methodology.

Declaration of Competing Interest

The authors declare that they have no known competing financial interests or personal relationships that could have appeared to influence the work reported in this paper.

Data availability

Data will be made available on request.

Acknowledgments

Appendix A. Supplementary material

Supplementary data to this article can be found online at https://doi.org/10.1016/j.bandc.2023.105969.

References

Arjona, A., Angulo-Ruiz, B. Y., Rodríguez-Martínez, E. I., Cabello-Navarro, C., & Gómez, C. M. (2023). Time-frequency neural dynamics of ADHD children and adolescents during a Working Memory task. *Neuroscience letters, 798*, 137100. Advance online publication. Doi: https://doi.org/10.1016/j.neulet.2023.137100.

Andre, J., Picchioni, M., Zhang, R., & Toulopoulou, T. (2015). Working memory circuit as a function of increasing age in healthy adolescence: A systematic review and meta-analyses. *NeuroImage Clinical, 12*, 940–948. https://doi.org/10.1016/j.nicl.2015.12.002

Bachman, M. D., & Bernat, E. M. (2018). Independent contributions of theta and delta time-frequency activity to the visual oddball P3b. *International journal of Psychophysiology: Official Journal of the International Organization of Psychophysiology, 128*, 70–80. https://doi.org/10.1016/j.ijpsycho.2018.03.010

Baddeley, A. (2012). Working memory: Theories, models, and controversies. *Annual Review of Psychology, 63*, 1–29. https://doi.org/10.1146/annurev-psych-120710-100422

Barriga-Paulino, C. I., Rodríguez-Martínez, E. I., Rojas-Benjumea, M.Á., & Gómez, C. M. (2014). Slow wave maturation on a visual working memory task. *Brain and Cognition, 88*, 43–54. https://doi.org/10.1016/j.bandc.2014.04.003

Barriga-Paulino, C. I., Rodríguez-Martínez, E. I., Rojas-Benjumea, M.Á., & Gómez González, C. M. (2015). Electrophysiological evidence of a delay in the visual recognition process in Young children. *Frontiers in Human Neuroscience, 9*, 622. https://doi.org/10.3389/fnhum.2015.00622

Barriga-Paulino, C. I., Rodríguez-Martínez, E. I., Arjona, A., Morales, M., & Gómez, C. M. (2017). Developmental trajectories of event related potentials related to working memory. *Neuropsychologia, 95*, 215–226. https://doi.org/10.1016/j.neuropsychologia.2016.12.026

Benjamini, Y., & Hochberg, Y. (1995). Controlling the false discovery rate: A practical and powerful approach to multiple testing. *Journal of the Royal Statistical Society, 57*, 289–300. https://doi.org/10.1111/j.2517-6161.1995. tb02031.x

Buzsaki, G. (2006). *Rhythms of the Brain.* New York: Oxford University Press.

Cohen, M. X. (2014). *Analyzing neural time series data: Theory and practice.* Cambridge, Massachusetts: The MIT Press.

Cordones, I., Gómez, C. M., & Escudero, M. (2013). Cortical dynamics during the preparation of antisaccadic and prosaccadic eye movements in humans in a gap paradigm. *PloS one, 8*(5), e63751.

Delorme, A., & Makeig, S. (2004). EEGLAB: An open source toolbox for analysis of single-trial EEG dynamics including independent component analysis. *Journal of Neuroscience Methods, 134*(1), 9–21. https://doi.org/10.1016/j.jneumeth.2003.10.009

Delorme, A., Sejnowski, T., & Makeig, S. (2007). Enhanced detection of artifacts in EEG data using higher-order statistics and independent component analysis. *NeuroImage, 34*(4), 1443–1449. https://doi.org/10.1016/j.neuroimage.2006.11.004

Gómez, C. M., Rodríguez-Martínez, E. I., Fernández, A., Maestú, F., Poza, J., & Gómez, C. (2017). Absolute power spectral density changes in the magnetoencephalographic activity during the transition from childhood to adulthood. *Brain topography, 30*(1), 87–97. https://doi.org/10.1007/s10548-016-0532-0

Gómez, C. M., Barriga-Paulino, C. I., Rodríguez-Martínez, E. I., Rojas-Benjumea, M.Á., Arjona, A., & Gómez-González, J. (2018). The neurophysiology of working memory development: From childhood to adolescence and young adulthood. *Reviews in the Neurosciences, 29*(3), 261–282. https://doi.org/10.1515/revneuro-2017-0073

Goncharova, I. I., McFarland, D. J., Vaughan, T. M., & Wolpaw, J. R. (2003). EMG contamination of EEG: Spectral and topographical characteristics. *Clinical Neurophysiology: Official Journal of the INTERNATIONAL Federation of Clinical Neurophysiology, 114*(9), 1580–1593. https://doi.org/10.1016/s1388-2457(03)00093-2

Groppe, D. M., Urbach, T. P., & Kutas, M. (2011). Mass univariate analysis of event-related brain potentials/fields I: A critical tutorial review. *Psychophysiology, 48*(12), 1711–1725. https://doi.org/10.1111/j.1469-8986.2011.01273.x

Harper, J., Malone, S. M., & Bernat, E. M. (2014). Theta and delta band activity explain N2 and P3 ERP component activity in a go/no-go task. *Clinical Neurophysiology: Official Journal of the International Federation of Clinical Neurophysiology, 125*(1), 124–132. https://doi.org/10.1016/j.clinph.2013.06.025

Heinrichs-Graham, E., & Wilson, T. W. (2015). Spatiotemporal oscillatory dynamics during the encoding and maintenance phases of a visual working memory task. *Cortex; A Journal Devoted to the Study of the Nervous System and Behavior, 69*, 121–130. https://doi.org/10.1016/j.cortex.2015.04.022

Hillyard, S. A., & Anllo-Vento, L. (1998). Event-related brain potentials in the study of visual selective attention. *Proceedings of the National Academy of Sciences of the United States of America, 95*(3), 781–787. https://doi.org/10.1073/pnas.95.3.781

Huttenlocher, P. R. (1990). Morphometric study of human cerebral cortex development. *Neuropsychologia, 28*(6), 517–527. https://doi.org/10.1016/0028-3932(90)90031-i

Jensen, O., & Mazaheri, A. (2010). Shaping functional architecture by oscillatory alpha activity: Gating by inhibition. *Frontiers in Human Neuroscience, 4*, 186. https://doi.org/10.3389/fnhum.2010.00186

Jenson, D., Bowers, A. L., Hudock, D., & Saltuklaroglu, T. (2020). The application of EEG Mu rhythm measures to neurophysiological research in stuttering. *Frontiers in Human Neuroscience, 13*, 458. https://doi.org/10.3389/fnhum.2019.00458

Kang, S. S., MacDonald, A. W., 3rd, Chafee, M. V., Im, C. H., Bernat, E. M., Davenport, N. D., & Sponheim, S. R. (2018). Abnormal cortical neural synchrony during working memory in schizophrenia. *Clinical Neurophysiology: Official Journal of the International Federation of Clinical Neurophysiology, 129*(1), 210–221. https://doi.org/10.1016/j.clinph.2017.10.024

Klimesch, W. (2012). α-band oscillations, attention, and controlled access to stored information. *Trends in Cognitive Sciences, 16*(12), 606–617. https://doi.org/10.1016/j.tics.2012.10.007

Koshy, S. M., Wiesman, A. I., Proskovec, A. L., Embury, C. M., Schantell, M. D., Eastman, J. A., … Wilson, T. W. (2020). Numerical working memory alters alpha-beta oscillations and connectivity in the parietal cortices. *Human Brain Mapping, 41*(13), 3709–3719. https://doi.org/10.1002/hbm.25043

Khursheed, F., Tandon, N., Tertel, K., Pieters, T. A., Disano, M. A., & Ellmore, T. M. (2011). Frequency-specific electrocorticographic correlates of working memory delay period fMRI activity. *NeuroImage, 56*(3), 1773–1782. https://doi.org/10.1016/j.neuroimage.2011.02.062

LaRocque, J. J., Lewis-Peacock, J. A., Drysdale, A. T., Oberauer, K., & Postle, B. R. (2013). Decoding attended information in short-term memory: An EEG study. *Journal of Cognitive Neuroscience, 25*(1), 127–142. https://doi.org/10.1162/jocn_a_00305

Lenartowicz, A., Delorme, A., Walshaw, P. D., Cho, A. L., Bilder, R. M., McGough, J. J., … Loo, S. K. (2014). Electroencephalography correlates of spatial working memory deficits in attention-deficit/hyperactivity disorder: Vigilance, encoding, and maintenance. *The Journal of Neuroscience: The Official Journal of the Society for Neuroscience, 34*(4), 1171–1182. https://doi.org/10.1523/JNEUROSCI.1765-13.2014

Lenartowicz, A., Truong, H., Salgari, G. C., Bilder, R. M., McGough, J., McCracken, J. T., & Loo, S. K. (2019). Alpha modulation during working memory encoding predicts neurocognitive impairment in ADHD. *Journal of Child Psychology and Psychiatry, and Allied Disciplines, 60*(8), 917–926. https://doi.org/10.1111/jcpp.13042

Lüchinger, R., Michels, L., Martin, E., & Brandeis, D. (2011). EEG-BOLD correlations during (post-)adolescent brain maturation. *NeuroImage, 56*(3), 1493–1505. https://doi.org/10.1016/j.neuroimage.2011.02.050

Maris, E., & Oostenveld, R. (2007). Nonparametric statistical testing of EEG- and MEG-data. *Journal of Neuroscience Methods, 164*(1), 177–190. https://doi.org/10.1016/j.jneumeth.2007.03.024

McKeon, S. D., Calabro, F., Thorpe, R. V., de la Fuente A.G., Foran, W., Parr A.C., Jones S. R. & Luna, B. (2023). Age-related change in transient gamma band activity during working memory maintenance through adolescence. *bioRxiv*, 2022.07.24.501317. Doi: https://doi.org/10.1101/2022.07.24.501317.

Oostenveld, R., Fries, P., Maris, E., & Schoffelen, J. M. (2011). FieldTrip: Open source software for advanced analysis of MEG, EEG, and invasive electrophysiological data. *Computational Intelligence and Neuroscience, 2011*, Article 156869. https://doi.org/10.1155/2011/156869

Ostby, Y., Tamnes, C. K., Fjell, A. M., & Walhovd, K. B. (2011). Morphometry and connectivity of the fronto-parietal verbal working memory network in development. *Neuropsychologia, 49*(14), 3854–3862. https://doi.org/10.1016/j.neuropsychologia.2011.10.001

Pelegrina, S., Molina, R., Rodríguez-Martínez, E. I., Linares, R., & Gómez, C. M. (2020). Age-related changes in selection, recognition, updating and maintenance information in WM. An ERP study in children and adolescents. *Biological Psychology, 157*, Article 107977. https://doi.org/10.1016/j.biopsycho.2020.107977

Polich, J. (2007). Updating P300: An integrative theory of P3a and P3b. *Clinical Neurophysiology: Official Journal of the International Federation of Clinical Neurophysiology, 118*(10), 2128–2148. https://doi.org/10.1016/j.clinph.2007.04.019

Postle, B. R. (2006). Working memory as an emergent property of the mind and brain. *Neuroscience, 139*(1), 23–38. https://doi.org/10.1016/j.neuroscience.2005.06.005

R Core Team (2020). R: A language and environment for statistical computing. R Foundation for Statistical Computing, https://www.R-project.org/.

Raghavachari, S., Kahana, M. J., Rizzuto, D. S., Caplan, J. B., Kirschen, M. P., Bourgeois, B., … Lisman, J. E. (2001). Gating of human theta oscillations by a working memory task. *The Journal of Neuroscience: the Official Journal of the Society for Neuroscience, 21*(9), 3175–3183. https://doi.org/10.1523/JNEUROSCI.21-09-03175.2001

Riddle, J., Scimeca, J. M., Cellier, D., Dhanani, S., & D'Esposito, M. (2020). Causal evidence for a role of theta and alpha oscillations in the control of working memory. *Current biology: CB, 30*(9), 1748–1754.e4. https://doi.org/10.1016/j.cub.2020.02.065

Rodríguez-Martinez, E. I., Barriga-Paulino, C. I., Zapata, M. I., Chinchilla, C., López-Jiménez, A. M., & Gómez, C. M. (2012). Narrow band quantitative and multivariate electroencephalogram analysis of peri-adolescent period. *BMC neuroscience, 13*, 104. https://doi.org/10.1186/1471-2202-13-104

Rosseel, Y. (2012). Lavaan: An R package for structural equation modeling. *Journal of Statistical Software, 48*(2), 1–36. http://www.jstatsoft.org/v48/i02/.

Ruchkin, D. S., Johnson, R., Jr, Canoune, H., & Ritter, W. (1990). Short-term memory storage and retention: An event-related brain potential study. *Electroencephalography and Clinical Neurophysiology, 76*(5), 419–439. https://doi.org/10.1016/0013-4694(90)90096-3

Sato, J., Mossad, S. I., Wong, S. M., Hunt, B. A. E., Dunkley, B. T., Smith, M. L., … Taylor, M. J. (2018). Alpha keeps it together: Alpha oscillatory synchrony underlies working memory maintenance in young children. *Developmental Cognitive Neuroscience, 34*, 114–123. https://doi.org/10.1016/j.dcn.2018.09.001

Sauseng, P., Klimesch, W., Heise, K. F., Gruber, W. R., Holz, E., Karim, A. A., … Hummel, F. C. (2009). Brain oscillatory substrates of visual short-term memory capacity. *Current Biology: CB, 19*(21), 1846–1852. https://doi.org/10.1016/j.cub.2009.08.062

Sauseng, P., Griesmayr, B., Freunberger, R., & Klimesch, W. (2010). Control mechanisms in working memory: A possible function of EEG theta oscillations. *Neuroscience and Biobehavioral Reviews, 34*(7), 1015–1022. https://doi.org/10.1016/j.neubiorev.2009.12.006

Segalowitz, S. J., Santesso, D. L., & Jetha, M. K. (2010). Electrophysiological changes during adolescence: A review. *Brain and Cognition, 72*(1), 86–100. https://doi.org/10.1016/j.bandc.2009.10.003

Tesche, C. D., & Karhu, J. (2000). Theta oscillations index human hippocampal activation during a working memory task. *Proceedings of the National Academy of Sciences of the United States of America*, 97(2), pp. 919–924. Doi: https://doi.org/10.1073/pnas.97.2.919.

Thornton, D., Harkrider, A. W., Jenson, D. E., & Saltuklaroglu, T. (2019). Sex differences in early sensorimotor processing for speech discrimination. *Scientific Reports, 9*(1), 392. https://doi.org/10.1038/s41598-018-36775-5

Vaquero, E., Gómez, C. M., Quintero, E. A., González-Rosa, J. J., & Márquez, J. (2008). Differential prefrontal-like deficit in children after cerebellar astrocytoma and medulloblastoma tumor. *Behavioral and Brain Functions: BBF, 4*, 18. https://doi.org/10.1186/1744-9081-4-18

Vázquez-Marrufo, M., Vaquero, E., Cardoso, M. J., & Gómez, C. M. (2001). Temporal evolution of alpha and beta bands during visual spatial attention. *Brain research. Cognitive Brain Research, 12*(2), 315–320. https://doi.org/10.1016/s0926-6410(01)00025-8

Whitford, T. J., Rennie, C. J., Grieve, S. M., Clark, C. R., Gordon, E., & Williams, L. M. (2007). Brain maturation in adolescence: Concurrent changes in neuroanatomy and neurophysiology. *Human Brain Mapping, 28*(3), 228–237. https://doi.org/10.1002/hbm.20273

Yaple, Z., & Arsalidou, M. (2018). N-back working memory task: meta-analysis of normative fMRI studies with children. *Child Development, 89*(6), 2010–2022. https://doi.org/10.1111/cdev.13080

Zammit, N., Falzon, O., Camilleri, K., & Muscat, R. (2018). Working memory alpha-beta band oscillatory signatures in adolescents and young adults. *The European Journal of Neuroscience, 48*(7), 2527–2536. https://doi.org/10.1111/ejn.13897

Zhou, X., Zhu, D., Katsuki, F., Qi, X. L., Lees, C. J., Bennett, A. J., Salinas, E., Stanford, T. R., & Constantinidis, C. (2014). Age-dependent changes in prefrontal intrinsic connectivity. *Proceedings of the National Academy of Sciences of the United States of America*, 111(10), pp. 3853–3858. Doi: https://doi.org/10.1073/pnas.1316594111.